

# Steady-state analysis and experimental evaluation of a resonant AC/DC converter for HF sinusoidal AC power distribution systems

MARCELO G. CENDOYA

Instituto de Investigaciones en Electrónica, Control y Procesamiento de Señales (LEICI)

Departamento de Electrotecnia, Facultad de Ingeniería

Universidad de La Plata

CC 91, La Plata 1900

ARGENTINA

cendoya@ing.unlp.edu.ar

*Abstract:* - The high frequency (HF) alternating current (AC) power distribution systems have significant advantages over their DC counterparts. This paper presents the analysis and experimental evaluation of an AC/DC resonant converter, suitable for use at the load side of HF sinusoidal AC power distribution systems. Foremost, a theoretical analysis of the converter operation in steady state and continuous conduction mode is performed. The analysis is focused on obtaining the conversion ratio, the distortion of the input current and the converter efficiency. In order to validate the theoretical analysis and to investigate the performance, a converter prototype was included in a laboratory HF sinusoidal AC distribution system. The experimental results present good correlation with predicted values obtained by means of calculations done with the mathematical expressions derived in the theoretical analysis. They also confirm the good performance of the converter for the suggested application.

*Key-Words:* - AC/DC resonant converter. HF AC power distribution systems.

## 1 Introduction

Currently, electric power distribution systems in direct current (DC) are used in applications such as: telecommunications systems, computers, satellites, space vehicles, cars, ships, among others. The constant search for greater efficiency and reliability was the driving force for the development of alternative systems, which consists in the use of an alternating current (AC) distribution bus with high operating frequency (HF). A good review on these systems can be found in the specialized literature [1]. In Fig. 1 the two basic architectures are shown, the DC distribution system (DC-DS) and the AC distribution system (AC-DS). It can be seen that the AC-DS has fewer conversion stages (a rectification and an inversion) and therefore, is potentially more efficient, has lower cost and would more reliable with respect to the DC-DS, due to its lower complexity and parts count [2]. It also presents the ease of changing the voltage level, using only one transformer. Although AC-DS has been investigated with square-wave AC buses, from the point of view of the EMI the use of sinusoidal AC buses is preferable [2]. As the attractive and promising results of the AC-DS, has motivated the development and study of new converter topologies

for their implementation that exploit their advantages at its maximum.

Although AC/DC converters for HF AC-DS can be found in the technical literature, most of them require bidirectional (V and I) switches [3] [4]. In addition, some of them use a somewhat complicated control scheme. In this article a resonant AC/DC converter was considered that has good characteristics for the use at the load side of an HF sinusoidal AC-DS. The main characteristics of the converter are:

- Wide range of variation of the output voltage.
- High input power factor (PF).
- Reasonable efficiency.
- Acceptable THD of the input current.

This last characteristic is very important, since it makes unnecessary the use of EMI filter at the converter input side to reduce the contamination of the AC bus with higher order harmonics. Another advantages are that the switch is on the converter DC side, which implies that only a unidirectional V/I device is required. In addition, the switch control scheme is very simple, requiring only synchronization with the zero crossing of the AC bus voltage.

The main objectives of the present work are the theoretical analysis of the aforementioned converter and its experimental evaluation to investigate the

validity of the analysis done and to know the converter performance in real different operating conditions. The paper is organized in the following manner: in Section 2 the converter and its principle of operation are described, in Section 3 the theoretical expressions for the determination of the output voltage, the harmonic distortion of the input current and the conversion efficiency are developed. Section 4 shows the experimental results compared to theoretical calculations and finally, in Section 5, some conclusions are pointed out.

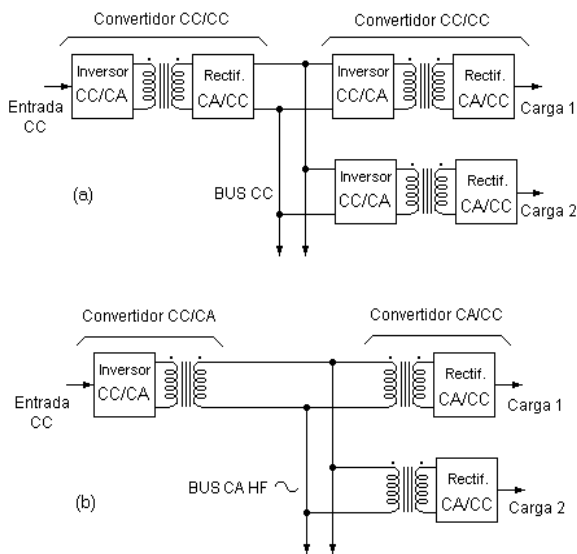


Figure 1. Distribution systems: (a) DC. (b) HF AC.

## 2 Converter description

The electrical circuit of the HF AC/DC resonant converter considered in the present article is presented in this section with a brief description of its principle of operation. The waveforms of the most salient magnitudes are also depicted.

### 2.1 Converter circuit

The electrical circuit of the converter under study is shown in Fig. 2. An input transformer links it to the AC bus. The transformer serves to adapt voltage levels and to give output isolation with respect to the AC bus lines. A capacitor ( $C_c$ ) in the secondary compensates the magnetization current to not degrade the input power factor (PF). Then, there is a series resonant circuit (LC) tuned for presenting an impedance null at the AC bus frequency, and a high impedance for other unwanted frequencies. This forces the input current to be practically sinusoidal (i.e. with low THD) and with a near unity displacement factor. This results in a high input

power factor (PF). Subsequently, the current is rectified by a full-wave diode bridge (D1-D4) whose output has a structure similar to that of a DC/DC boost converter. That is, a power switch (M1), in this case a MOSFET device, derives some of the rectifier bridge output current to ground controlling the portion of it that reaches the load; a series diode (D5) and an output filter capacitor ( $C_s$ ) in parallel with the load resistance ( $R_L$ ).

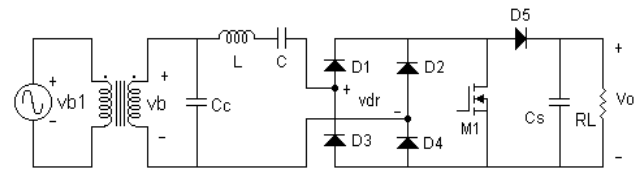


Figure 2. HF resonant AC/DC converter circuit.

### 2.2 Converter principle of operation

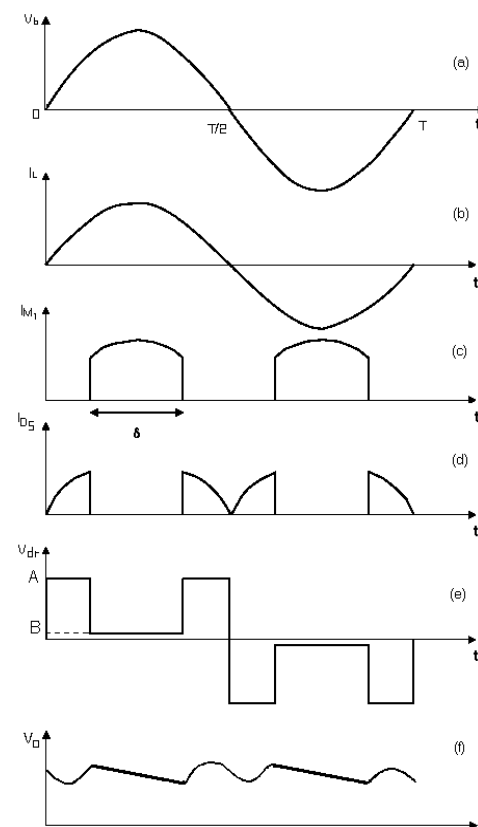


Figure 3. Idealized converter waveforms: (a) Transformer secondary voltage ( $V_{b2}$ ) (b) Inductor current ( $I_L$ ) (c) Switch current ( $I_{M1}$ ) (d) Diode D5 current ( $I_{D5}$ ) (e) Bridge rectifier input voltage ( $V_{dr}$ ) (f) Output voltage ( $V_o$ )

The waveforms of the most relevant electrical magnitudes of the converter operating in steady-state and continuous conduction mode (CCM), are sketched in Fig. 3. The switch M1 is turned-on during the conduction angle  $\delta$ . During the M1 on-state, D5 is reversed polarized by the output voltage. Then, the resonant current when circulating through M1 causes the voltage at the input of bridge D1-D4 to be approximately zero. This increases the quality factor of the resonant circuit (Q) and a greater energy is stored in its reactive elements. Meanwhile,  $C_S$  is discharged in  $R_L$  so that the output voltage drops in an approximately linear fashion. When M1 is open the resonant current will circulate through D5 and the instantaneous input voltage of the rectifier bridge is approximately equal to  $V_o$  or  $-V_o$  depending on the input current direction. The Q decreases and the excess stored energy is delivered to  $R_L$  and  $C_S$ , replenishing its charge. The output ripple in that section has a pseudo-sinusoidal shape.

### 3 Converter analysis in steady-state

In this section a theoretical analysis of the converter is presented. The analysis will be performed in steady-state operation with continuous conduction mode (CCM). This operation mode refers that the input current is not extinguished at any time (except in the zero crossing, of course). To do this, a sufficient inductance value must be used. The analysis is focused on obtaining the average output voltage (i.e., the conversion ratio), the total harmonic distortion (THD) of the input current and the converter efficiency.

#### 3.1 Conversion ratio

To obtain the dependency of the converter output voltage with  $\delta$ , we can apply the sinusoidal analysis technique for resonant converters [5]. This technique basically consists in considering the fundamental components of the involved non-sinusoidal electrical quantities. We will assume that the converter operates in CCM, and that the HF AC bus voltage is purely sinusoidal. Then, it is true that:

$$\hat{V}_b = \hat{V}_{dr1} + r_b \hat{I}_b \quad (1)$$

, where

$\hat{V}_b$ : HF AC bus voltage, peak value.

$\hat{V}_{dr1}$ : Bridge rectifier fundamental input voltage, peak value.

$\hat{I}_b$ : AC bus current, peak value.

$r_b$ : LC network total series parasitic resistance.

By performing the Fourier analysis of  $V_{dr}$ , shown in Fig. 3 (e), we obtain:

$$\hat{V}_{dr1} = \frac{4}{\pi} \{ A [1 - \text{sen}(\delta/2)] + B \text{sen}(\delta/2) \} \quad (2)$$

where  $A$  corresponds to the high value and  $B$  to the low value:

$$\begin{aligned} A &= V_o + 3V_\gamma \\ B &= 2V_\gamma \end{aligned} \quad (3)$$

$\hat{I}_b$  can be obtained through the power balance:

$$P_o = \eta P_i \rightarrow \hat{I}_b = \frac{2V_o^2}{\eta \hat{V}_b R_L} \quad (4)$$

From (1), (2), (3) and (4) results:

$$\begin{aligned} \frac{\pi r_b}{2\eta R_L \hat{V}_b} V_o^2 + [1 - \text{sen}(\delta/2)] V_o + \\ + V_\gamma [3 - \text{sen}(\delta/2)] - \frac{\pi}{4} \hat{V}_b = 0 \end{aligned} \quad (5)$$

In many cases  $r_b$  is small enough that the second order term in (5) can be neglected. In that situation, the conversion ratio will be given by:

$$V_o \cong \frac{\frac{\pi \hat{V}_b}{4} - V_\gamma [3 - \text{sen}(\delta/2)]}{[1 - \text{sen}(\delta/2)]} \quad (6)$$

From (6) can be seen that the greater  $\delta$ , more output voltage is obtained.

#### 3.2 Input current harmonic distortion

Looking at Fig. 3 (e), it is easy to see that the input voltage of the bridge rectifier has a strong third harmonic component. For this reason, the distortion of the input current will be determined virtually by this component. It is given by:

$$I_{3ef} = \frac{\hat{V}_{dr3}}{\sqrt{2}Z_3} \quad (7)$$

, where

$\hat{V}_{dr3}$ :  $V_{dr}$  third harmonic, peak value

$Z_3 = 3\omega_o L - 1/3\omega_o C$  with  $\omega_o = 1/\sqrt{LC} = 2\pi f_b$

Applying Fourier analysis to the input voltage of the bridge rectifier, we obtain:

$$\hat{V}_{dr3} = \frac{4}{3\pi} \{A[1 + \text{sen}(3\delta/2)] - B\text{sen}(3\delta/2)\} \quad (8)$$

The, the total harmonic distortion of the input current (THD) is approximately given by:

$$\begin{aligned} THD[\%] &\cong \frac{I_{3ef}}{I_{bef}} \times 100 = \\ &= \frac{200\eta\hat{V}_b R_L}{3\pi V_0^2 Z_3} \{A[1 + \text{sen}(3\delta/2)] - B\text{sen}(3\delta/2)\} \end{aligned} \quad (9)$$

### 3.2 Efficiency

Evaluating the losses in the diodes, the MOSFET and the LC circuit, results:

$$\begin{aligned} P_{perdidas} &= I_{bef}^2 r_b + I_{M1ef}^2 R_{ON} + \\ &+ P_{swM1} + 4\bar{I}_{b/2ciclo} V_\gamma + \bar{I}_{D5} V_\gamma \end{aligned} \quad (10)$$

Introducing (10) in the efficiency equation:

$$\eta = \frac{P_o}{P_o + P_{perdidas}} \Rightarrow \eta^2 + C_1\eta + C_2 = 0 \quad (11)$$

with:

$$\begin{aligned} C_1 &= \frac{4}{\hat{V}_b} \left\{ \frac{t_{SW} V_0}{T} \cos(\delta/2) + \frac{V_\gamma}{\pi} [3 - \text{sen}(\delta/2)] \right\} - 1 \\ C_2 &= \frac{2V_0^2}{R_L \hat{V}_b^2} \left\{ \frac{R_{ON}}{\pi} [\delta + \text{sen}(\delta)] + r_b \right\} \end{aligned} \quad (12)$$

, where:

$t_{SW} = t_{SWon} + t_{SWoff}$ : MOSFET switching time.

$T = 1/f_b$ : AC bus voltage time period.

$R_{ON}$  = MOSFET conduction resistance.

To calculate the coefficients given in (12), it is necessary to know the value of  $V_o$ , which can be calculated by (5). Unfortunately to evaluate (5) it is necessary to know the efficiency, therefore an equations system must be solved. It is noted that, for a given HF AC bus (voltage and frequency), the efficiency depends on the working point, defined by  $\delta$  and  $R_L$ .

## 4 Experimental results

### 4.1 Description of the experimental setup

To evaluate the performance of the converter, it was included in an experimental HF sinusoidal AC distribution system, depicted in Fig 4. The generation of the bus voltage was obtained using a

single-phase inverter with a phase-shifted PWM method, giving a single pulse voltage waveform with a rated width of  $120^\circ$  to minimize the third harmonic component. The quasi-square output voltage of an "H" bridge of four MOSFETs is filtered with a high Q series-parallel LC network. Well known procedures and guidelines were followed for the inverter design [6]. The low distortion sinusoidal AC bus voltage is  $V_{bef} = 25V$  with a frequency of  $f_b = 20KHz$ . The values of the resulting circuit elements are:  $L_s = 721.4\mu Hy$ ;  $C_s = 87.7nF$ ;  $L_p = 229.1\mu Hy$ ;  $C_p = 276.4nF$ ;  $V_{CC} = 34,5V$ ;  $S_{1-4} = IRF530$ .

A resonant AC/DC converter prototype was designed to meet the following basic requirements:  $P_o = 50W$ ;  $V_o = 48V$ ;  $\delta = 60^\circ$ ;  $46\Omega < R_L < 100\Omega$ ,  $THD < 10\%$ ;  $v_{rppmax} = 2\%$ .

The values of the resulting converter components were:  $M_1 = IRF530$ ;  $D_{1-5} = MUR420$ ;  $L = 649.9\mu Hy$ ;  $C = 97.4nF$ ;  $r_b = 1,76\Omega$ ;  $C_s = 100\mu F$ ;  $C_c = 65nF$ ;  $L_m = 972.8\mu Hy$ , Transformer turns ratio: 1:1.

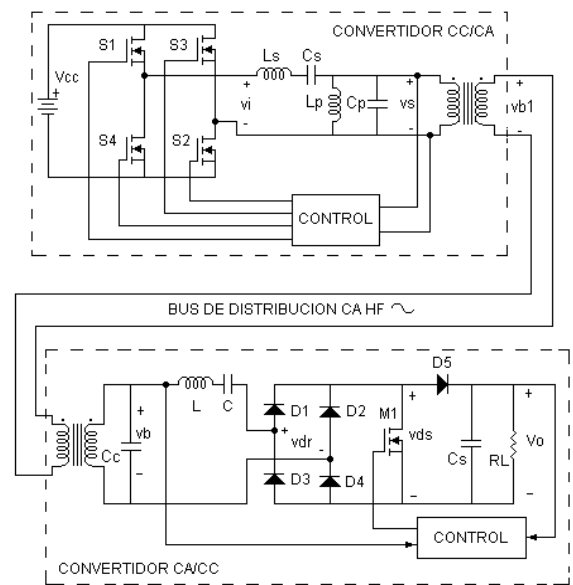


Figure 4. Experimental HF AC distribution system.

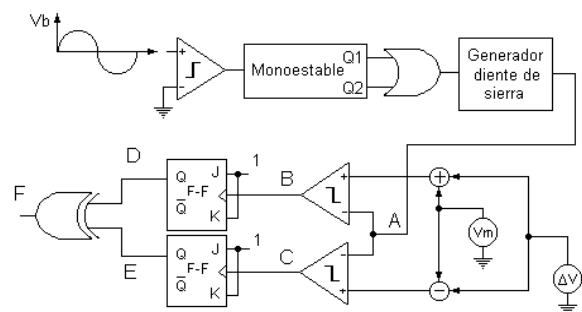


Figure 5. Converter control circuit.

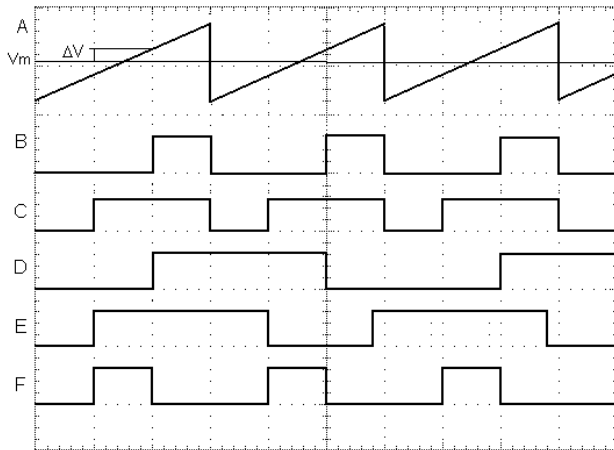


Figure 6. Control circuit waveforms.

In the absence of a suitable commercial IC to generate the control signal for the MOSFET switch, a circuit was designed for this purpose, whose block diagram is presented in Fig. 5. The waveforms of the fundamental signals of the control circuit are shown in Fig. 6. The circuit generates a compatible TTL level signal (F) with continuously variable width  $\delta$  as a function of a DC value  $\Delta V$ . This signal feed a MOSFET gate driver IC, type IR2121.

## 4.2 Test results

### 4.2.1 Validation of the theoretical operation

In order to corroborate if the converter operates as predicted by the theoretical analysis presented in Section 3, in a first step the waveforms of the most salient electrical magnitudes of the converter were examined.

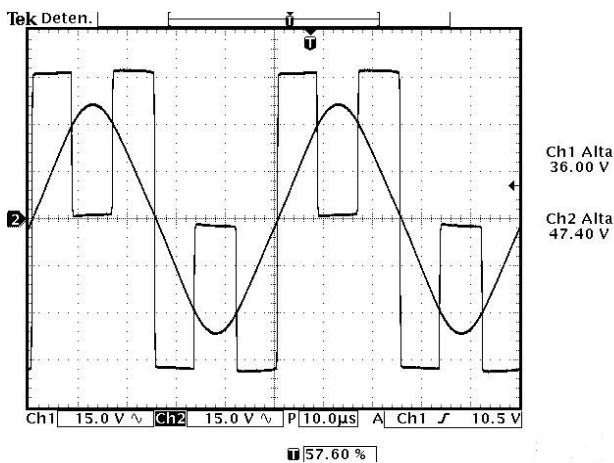


Figura 7.  $V_b$  y  $V_{dr}$ . Scale: 15V/div.

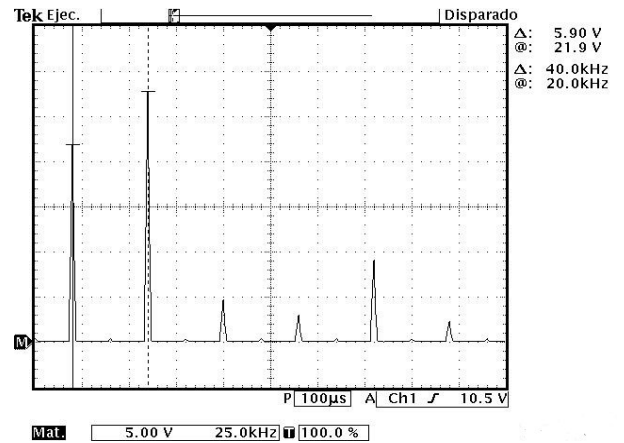


Figure 8.  $V_{dr}$  Spectrum.

In Fig. 7 the waveform of  $V_{dr}$  is shown next to that of bus  $V_b$ . The  $V_{dr}$  spectrum is shown in Fig. 8, where a relatively strong third harmonic content (responsible for the THD of the input current) is appreciated. The voltage difference between the fundamental component of  $V_{dr}$  and the bus voltage is the voltage drop in the parasitic resistance of the LC tank,  $E_c$ . 1. The obtained values satisfy approximately the same, since they are  $V_{dr_{ief}}=21,9V$ ,  $V_{bef}=25V$ ,  $I_{bef}=1,13A$  and  $r_b=1.76\Omega$ . In Fig. 9 the currents are shown by diode D5 and by the MOSFET. The oscilloscope screenshots of Fig. 7 and Fig.9 show a good agreement with the idealized waveforms of Fig.3.

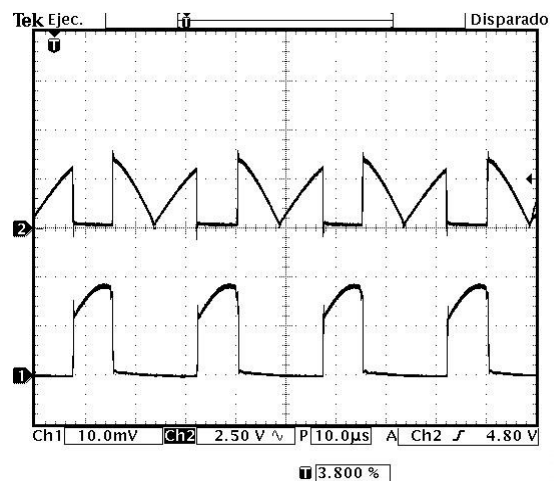


Figure 9.  $I_{D5}$  and  $I_{M1}$ . Scale: 1A/div.

### 4.2.2 Evaluation of the converter performance

As the theoretical analysis has focused on obtaining the output voltage, the input current THD and the efficiency of the converter, the results of the measurements of these important characteristics are shown below.

**Conversion ratio**

The average output voltage was measured for different conduction angles, for maximum (100Ω) and minimum load (35Ω, slightly lower than rated minimum to simulate a temporary overload). In the latter case  $\delta$  was reduced to 40° in order to not exceed the absolute maximum ratings of the converter components. Table I compares the results obtained with the values calculated by Eq. 5, considering  $V\gamma=0.7V$ , an average efficiency of 75% and a transformer with 1:1 turns ratio.

$\delta [^\circ]$	$R_L [\Omega]$	$V_o [V]$	
		Calculated	Measured
30	100	33.4	33.6
60	100	47.6	46.2
30	35	31.2	32.4
40	35	34.3	33.9

Table 1. Calculated and measured output voltage.

**Output ripple**

Fig. 10 shows the ripple in  $V_o$  and the gate signal of the MOSFET to have a time reference of when it is ON. The test was carried out in the most unfavourable situation ( $\delta=60^\circ$  and  $R_L=60\Omega$ ). It is observed that the ripple peak-to-peak amplitude (0.4V) is below the specified one (2% of  $48V=0.96V$ ) this is due to the fact that was employed a  $C_s$  capacitor of commercial value, higher than necessary.

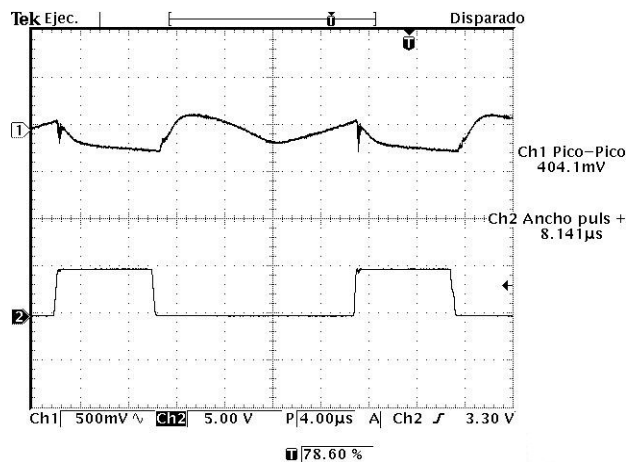


Figure 10.  $V_o$  ripple and  $V_{Gate}$  ( $R_L=60\Omega$  y  $\delta=60^\circ$ ) Scales: 0.5V/div y 5V/div.

**Input current THD**

Since the THD of  $I_b$  depends on the converter operating point, the values obtained for two working conditions are shown, which correspond to  $THD_{max}$  and  $THD_{min}$ , respectively. The current of the bus  $I_b$  and its corresponding spectrum for  $THD_{max}$  ( $R_L=100\Omega$  y  $\delta=30^\circ$ ) are shown in Fig. 11 and Fig. 12. In Fig. 13 and Fig. 14 the bus current and its spectrum are shown, for:  $THD_{min}$  ( $R_L=35\Omega$  y  $\delta=40^\circ$ ). It can be seen in both cases that the zero crossing of the input current of the converter practically coincides with that of the bus voltage. In Table 2, the measured THD is compared with calculated by means of Eq. 9, considering an average efficiency of 75% and knowing that the AC bus has  $\hat{V}_b=35.35V$ .

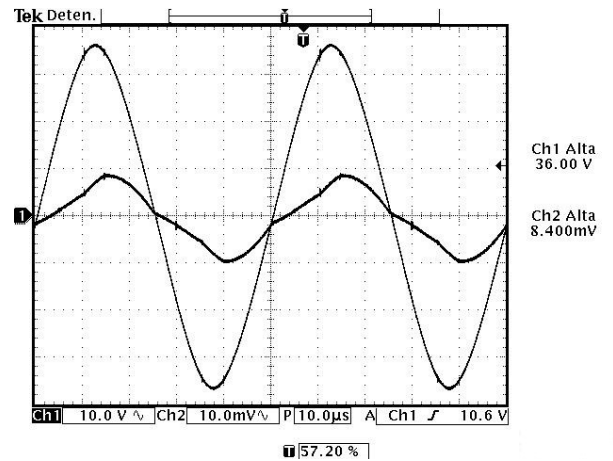


Figure 11.  $V_b$  and  $I_b$  ( $R_L=100\Omega$  y  $\delta=30^\circ$ ) Scales: V: 10V/div, I: 1A/div

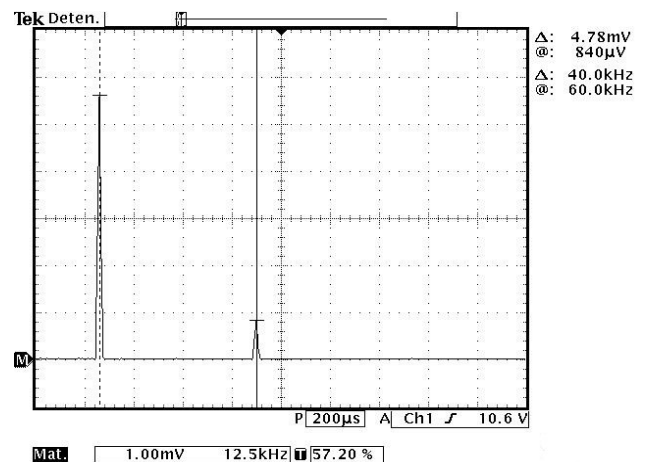


Figure 12. Spectrum for  $I_b$  of Fig. 11, THD=14.9%.

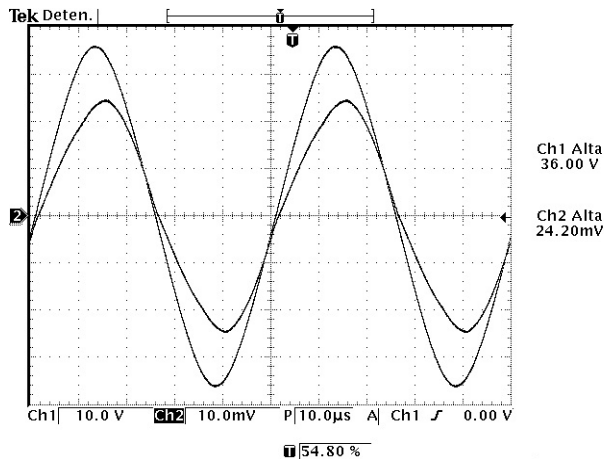


Figure 13.  $V_b$  and  $I_b$  ( $R_L=35\Omega$  y  $\delta=40^\circ$ )  
Scales: V: 10V/div , I: 1A/div

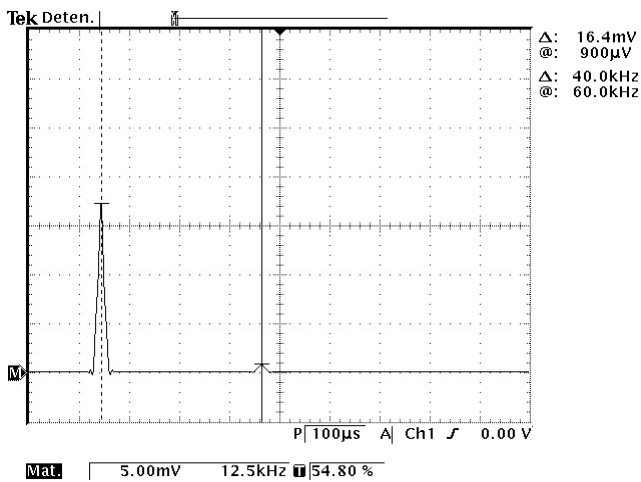


Figure 14. Spectrum of  $I_b$  of Fig.13.  
THD = 5.2%.

$R_L$ [ $\Omega$ ]	$\delta$ [ $^\circ$ ]	THD [%]	
		Calculated	Measured
100	30	14.7	14.9
35	40	5.5	5.2

Table 2: Calculated and measured THD of  $I_b$

Conversion efficiency

Finally, the efficiency of the converter was measured in four operating conditions. The results are shown in Table 3, together with the values calculated with Eq. 11 considering:  $t_{sw}=1\mu s$ ,  $T=50\mu s$ ,  $R_{ON}=0.142\Omega$ ,  $R_b=1.76\Omega$  and  $V_o$  obtained

by the Eq. 5. Since Eq. 5 also depends on the efficiency, it should be solved simultaneously with Eq. 11. However, to simplify the calculation process, an average efficiency of 75% was considered to evaluate Eq.5.

$R_L$ [ $\Omega$ ]	$\delta$ [ $^\circ$ ]	$\eta$ [%]	
		Calculate d	Measured
100	30	81.8	80.7
100	60	75.5	77.3
35	30	75.5	77.2
35	40	72.2	75.3

Table 3: Calculated and measured efficiency.

**5 Conclusions**

In the present work, an AC/DC resonant converter suitable to be used in AC distribution systems with HF sinusoidal voltage buses was considered. The converter was analysed and evaluated experimentally in a laboratory set up. The following conclusions can be highlighted:

- 1) Analytical expressions were deduced for the conversion ratio, the THD of the input current and the efficiency of the converter.
- 2) The values calculated with the theoretical expressions showed good agreement with the measured ones in the experimental set-up.
- 3) The input current has an acceptable harmonic distortion on the entire range of operation.
- 4) The converter showed a somewhat lower efficiency, but one must consider that was obtained with an experimental prototype whose design was not optimized. Surely it can be improved with a better design method.

Finally, and as a global conclusion, it can be said that the experiments results confirm that the resonant converter considered in this article presents a fairly good behaviour for the suggested application. Its salient points are: high input PF, wide range of variation of the output voltage, EMI filter is not required, necessitates only an unidirectional (V and I) switch and simple control scheme.

*References:*

- [1] P. Jain, M. Pahlevaninezhad, S. Pan, J. Drobnik, *A Review of High-Frequency Power Distribution Systems: for Space, Telecommunication, and Computer Applications*, IEEE Trans. on Power Electronics, Vol. 29, Issue: 8, pp. 3852–3863, Aug. 2014.
- [2] S. Luo, W. Gu, I. Batarseh and T. Wu, *Investigation of candidate techniques for high-frequency AC distributed power systems*, 43rd IEEE Midwest Symposium on Circuits and Systems, Lansing MI, 650-653, 2000.
- [3] J. Zeng, X. Li, J. Liu, *A Controllable LCL-T Resonant AC/DC Converter for High Frequency Power Distribution Systems*, Journal of Power Electronics 15(4):876-885, July 2015.
- [4] F. Musavi, P.K. Jain, H. Zhang, *A current controlled AC/DC converter for high frequency power architecture*, in Proceedings of the 33rd Annual IEEE Power Electronics Specialists Conference, Cairns, Qld., Australia, 2002.
- [5] R.W. Erickson and D. Maksimovic, *Fundamentals of Power Electronics*, 2nd Ed., Kluwer Academic Publishers, USA, 2001.
- [6] M.C. Tanju and P.K. Jain, *A 20KHz Hybrid Resonant Power Source for the Space Station*, IEEE Trans. on Aerospace and Electronic Systems, 25, 491-496, 1989.